Artery and Vein Diameter Ratio Measurement Based on Improvement of Arteries and Veins Segmentation on Retinal Images

Yuji Hatanaka, *Member, IEEE*, Hirokazu Tachiki, Kazunori Ogohara, Chisako Muramatsu, Susumu Okumura, and Hiroshi Fujita, *Member, IEEE*

Abstract— **Retinal arteriolar narrowing is decided based on the artery and vein diameter ratio (AVR). Previous methods segmented blood vessels and classified arteries and veins by color pixels in the centerlines of blood vessels. AVR was definitively determined through measurement of artery and vein diameters. However, this approach was not sufficient for cases with close contact between the artery of interest and an imposing vein. Here, an algorithm for AVR measurement via new classification of arteries and veins is proposed. In this algorithm, additional steps for an accurate segmentation of arteries and veins, which were not identified using the previous method, have been added to better identify major veins in the red channel of a color image. To identify major arteries, a decision tree with three features was used. As a result, all major veins and 90.9% of major arteries were correctly identified, and the absolute mean error in AVRs was 0.12. The proposed method will require further testing with a greater number of images of arteriolar narrowing before clinical application.**

I. Introduction

Funduscopy is an effective noninvasive method to diagnose diabetic retinopathy and glaucoma through direct observation of the blood vessels in the retina. Other than eye diseases, funduscopy can also be used to diagnose systemic hypertension by estimating cerebrovascular status, owing to the close proximity of the retina to the brain. Moreover, funduscopic examination of the retina can be useful in other medical fields, including ophthalmology, neurosurgery, and cardiology.

Retinal images are interpreted based on Keith–Wagner classification or Scheie classification of hypertensive retinopathy. The Scheie classification system grades retinopathy into two categories: hypertensive changes and arteriosclerotic changes, in which signs of low-grade diseases are related to blood vessels and grades 1 and 2 are determined based on the degree of arteriolar narrowing and scored according to the retinal artery and vein diameter ratio (AVR). Decreasing AVR is associated with an increased risk of stroke and myocardial infarction.

Studies of the association of retinopathy and blood vessel segmentation have arrived at the following consensus of four categories of blood vessel segmentation algorithms [1–4]: (i) matched filtering [1], (ii) a multi-scale method [2, 3], (iii) a supervised method [3], and (iv) morphological processing [4]. Chaudhuri et al. proposed a method using twelve different templates that were used to search for vessel segments along all possible directions [1]. Rangayyan et al. used multi-scale Gabor filter, coherence, and the green channel of pixel value as features, and it classified pixels using multilayer perceptron [2]. Niemeijer et al. developed a system to grade blood vessels using the k-nearest neighbor classifier with a multi-scale Gaussian-matched filter and its first and second order derivatives [3]. We also proposed a method employing a combination of a double-ring filter and black top-hat (BTH) transformation [4]. Double-ring filter is composed of the inner and outer ring regions, resulting in fast outputs with the contrast based on differences between the mean values of these regions.

We have reported for grading of hypertensive changes based on measurements of the diameters of arteries and veins [4, 5]. In this system, the arteries and veins are classified according to linear discriminant analysis (LDA) of eight pixel-based-features in the centerline of the candidate blood vessel [4]. Niemeijer et al. also proposed an AVR measurement method by classifying the arteries and veins based on color pixels in the centerlines of blood vessels [6]. Vázquez et al. [7] proposed a classification method based on a minimal path approach, where the vessels are segmented, measured, and classified according to several circumferences concentric to the optic disc. These vessel segments are then tracked and final results are obtained via a voting technique. However, these methods were not thought about segmentation of artery neighboring a vein as shown in Fig. 1. Therefore, the purpose of this study was to reconstruct the AVR measurement algorithm by improving classification of candidate arteries and veins.

II. Methods

A. Previous AVR measurements

The AVR measurement zone was designated as between the quarter-disc and one-disc diameters from the optic disc margin, in accordance with the methods of a previous Japanese study (Fig. 2) [4]. AVR is generally determined using the six largest arteries and veins on retinal images centered at the optic disc [8]. However, the retinal images for screening exams are obtained with the center of macula for

* This research was supported by grants from the Telecommunications Advancement Foundation and JSPS KAKENHI Grant Numbers 16K01415 and 26108005.

Y. Hatanaka and K. Ogohara are with the Department of Electronic Systems Engineering, School of Engineering, the University of Shiga Prefecture, 2500 Hassaka-cho, Hikone-shi, Shiga 522-8533, Japan (phone: 81-749-28-9556; fax: 81-749-28-9576; e-mail: hatanaka.y@usp.ac.jp).

H. Tachiki is a graduate student in the Division of Electronic Systems Engineering, Graduate School of Engineering, The University of Shiga Prefecture, 2500 Hassaka-cho, Hikone-shi, Shiga 522-8533, Japan.

S. Okumura is with the Department of Mechanical Systems Engineering, School of Engineering, The University of Shiga Prefecture, 2500 Hassaka-cho, Hikone-shi, Shiga 522-8533, Japan.

C. Muramatsu and H. Fujita are with the Department of Intelligent Image Information, Graduate School of Medicine, Gifu University, 1-1 Yanagido, Gifu-shi, Gifu 501-1194, Japan.

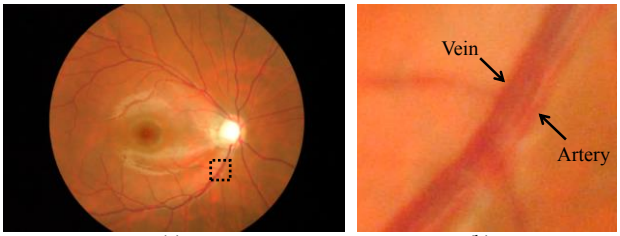

Figure 1. A representative image of an artery and a vein in close contact. (b) Enlarged image of the blood vessel marked by a rectangle in (a).

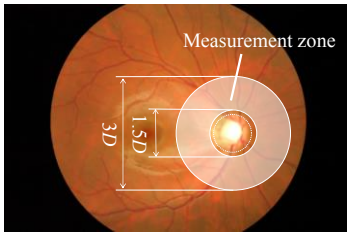

Figure 2. Determination of an AVR measurement zone. *D*, optic disc diameter.

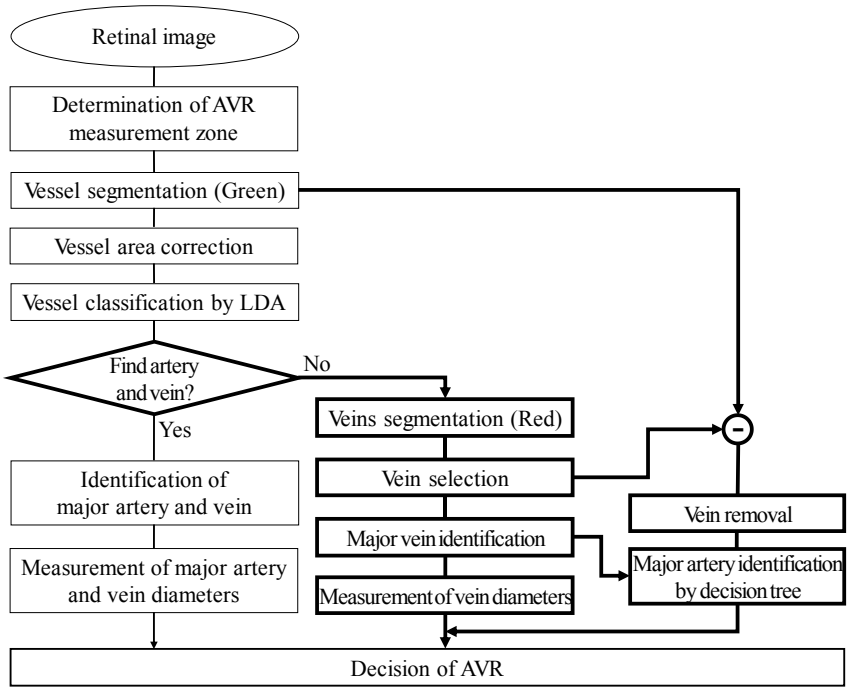

Figure 3 Flowchart of AVR measurement. Thin line boxes show processes by previous method. Bold line boxes show processes added by our proposed method.

screening various diseases. Therefore, it may be more reliable to the temporal vessels for the AVR measurement in such images. In our previous method, indicated by thin lines in Fig. 3, optic disc location and approximate diameters were determined using an active contour method for determination of the AVR measurement zone [9]. The blood vessel regions were segmented by combining a double-ring filter and BTH transformation in the green channel of color retinal images [4]. However, the contrast of some of the blood vessel segments was low; therefore, in some instances, the vessels were separated, as shown in Fig. 4 (a). The resulting gap was interpolated by template-matching using a blood vessel model [5]. Using reflected and non-reflected blood vessels as references, two blood vessel models were created, as shown in Fig. 4 (b) and (c). Pixel distribution of the blood vessel region of the model was Gaussian. By setting three diameters (9, 13, and 17 pixels) and 3 pixel densities (5, 9, and 13 in 8 bit), total 18 types of models were used. Representative template-matched and corrected images are shown in Fig. 4 (d) and (e), respectively. Crossing-points and bifurcations of the blood vessels were well depicted by the number of pixels (NoP) on the centerlines. Where, NoP = 3 was defined as a

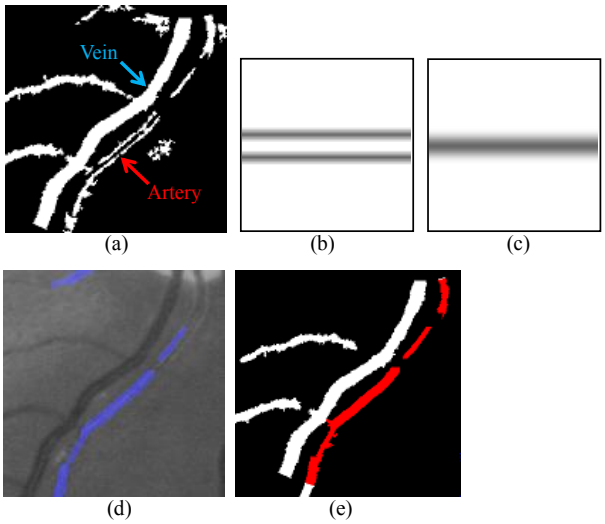

Figure 4 Vessel correction by template-matching. (a) An example of initial blood vessels segmentation. (b) Blood vessel model for reflected one. (c) Blood vessel model for non-reflected one. (d) Result of template-matched image. (e) Result of blood vessel correction.

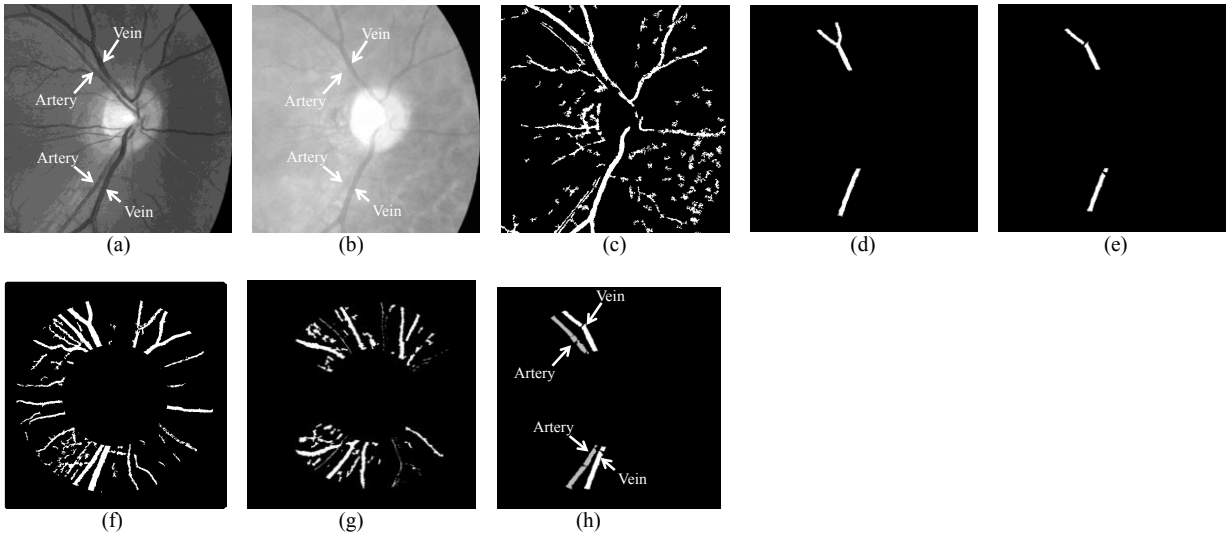

Figure 5. Result of major artery and vein identification with these added processes. (a) Green component image. (b) Red component image. Contrasts of arteries were lower than (a). (c) Vein candidates extracted in (b). (d) Vein candidates identified. (e) Final major vein identified. (f) Blood vessels extracted in (a). (g) Artery candidates identified by removing vein. (h) Final major arteries and man veins identified.

bifurcation and NoP = 4 was defined as a crossing-point. The candidate veins were divided into branch segments at crossing-points and bifurcations. Centerlines of candidate blood vessels were then detected using the Hilditch thinning algorithm. The pixels on the centerline were classified as an artery or a vein using LDA. Eight features of artery-vein properties were used for classification: the three original color components (red, green, and blue), three contrasts in the color channels, and outputs of the double-ring filter and BTH transformation. In this study, a temporal arteries and veins were identified, because the optic disc and the macula appeared symmetrical in the images. The small blood vessel segments were then removed and those within the limits of experimentally determined direction were identified as candidates of arteries and veins. If length of branch was under a half of the optic disc diameter, the branch was found by using new process. The vessel diameters were determined by the length of the shortest path through the centerline pixels inside the vessel region. Artery width W_{Ai} and vein one W_{Vj} were defined as means of these widths. AVR was finally calculated by using equation (1).

$$\mathrm{AVR} = \frac{\sum_{i=0}^{n} W_{\mathrm{A}i} / n}{\sum_{j=0}^{m} W_{\mathrm{V}j} / m} \qquad (1)$$

where "n" and "m" present the number of artery and vein branches, respectively. "n" and "m" were maximum 2 in this study [10].

B. Novel process for candidate artery and vein identification

In a preliminary test, our previous method failed to correctly identify approximately 25% of arteries. Thus, we added processes for the identification of such arteries, as illustrated by the bold lines in Fig. 3. It is well known that absorbance of oxygenated hemoglobin is significantly lower than that of reduced hemoglobin in the red light band (600-750 nm). In the red component of the color image shown in Fig. 5 (a) and (b), contrast of the arteries is very low because of the abundance of oxygenated hemoglobin in arterial blood.

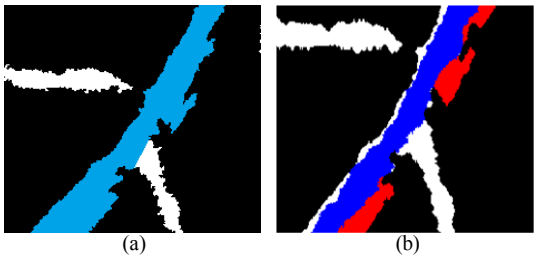

Figure 6. Result of major artery and vein segmentation by our previous method and added processes. Blue and red indicate identified areas of veins and arteries, respectively. (a) Results of our previous method. (b) Results of our proposed method.

1) Major vein identification

Candidate veins were segmented using our previous method in the red component of a color retinal image. However, the red component contained considerable noise in parts of artery, as depicted in Fig. 5 (c). Thus, small candidates were removed to ameliorate the noise. The veins were identified using LDA with the eight features proposed in our previous method [4]. A representative image of the identified vein is shown in Fig. 5 (d). To identify major veins for AVR measurement, vein candidates were divided into branch segments at crossing-points and bifurcations. In general, if several candidate veins run parallel, the widest should be chosen as the major vein, as shown in Fig. 5 (e).

2) Major artery identification

A representative image of candidate blood vessels detected in the green channel of color images is shown in Fig. 5 (f). By excluding the vein described above as a vessel candidate, the artery candidates were obtained, as shown in Fig. 5 (g). Major arteries were identified according to a decision tree [11] with three features. Differences in the mean diameter and area of

the artery of interest and the next candidate were defined as two features. A third feature was the angle using three points: the centers of the artery of interest, the optic disc, and the closest major vein. Fig. 5 (h) shows the final identification of the major arteries and major veins for AVR measurement. For the case presented in Fig. 1, although the previous method was insufficient to identify a major artery and a major vein, the added processes described in the flowchart facilitated successful segmentation, as shown in Fig. 6.

III. Results

The 22 retinal images used in this study were obtained in a university hospital using a Nonmyd 7 digital retinal camera (Kowa Medical, Aichi, Japan). These were images used in our previous study [5]. The images were saved in JPEG format at a resolution of 3008 × 2000 pixels. The created database includes each of the 44 major arteries and major veins. The focus of this study was to identify major arteries and veins for AVR measurement. The blood vessels were selected from manual segmentation results and definitively classified as either arteries or veins by an ophthalmologist. On the basis of these definitively classified images, the vessel diameters in the measurement zones were automatically calculated. For this purpose, the optic disc centers and diameters were manually identified.

Based on our previous method [5], 93.2% (41/44) of the major veins and 75.0% (33/44) of the major arteries were identified. In addition, all of three major veins and 7 of the remaining 11 major arteries were correctly identified using the process described in section II B. In the preliminary test, we compared decision tree and random forest for selection of major arteries. We applied decision tree which is simpler than random forest because these show the same ability.

The absolute mean error and standard deviation of AVR based on our proposed method were 0.12 and 0.077, whereas they were 0.094 and 0.070 based on our proposed method. Our previous method could not calculate AVR in two images, but our proposed method calculated AVR in all images. Our proposed method could identify seven arteries and 3 veins, which were not identified by our previous method. However, the accuracy of such blood vessels segmentation was low. Therefore, we continue with the development of a new blood vessel segmentation system based on high-order local autocorrelation, which performed better in blood vessel segmentation than the method proposed in this study [12]. Moreover, we proposed a vein diameter measurement based on correction of the vessel centerline and walls in arteriovenous crossing to improve the performance of blood vessel diameter measurement [13]. The method is able to measure the vein diameters with 1.39 pixels mean error. Applying these methods would make better the performance of AVR measurement.

IV. Conclusion

This paper described an improvement to AVR measurement via separate identification of major arteries and major veins. All major veins and 90.9% of major arteries were correctly identified. As a result, the absolute mean error in the AVRs was 0.12. The proposed method will require further testing with a greater number of images of arteriolar narrowing before clinical application.

Acknowledgment

The authors thank A. Mizukami, T. Iwase, A. Aoyama, and T. Yamamoto for their significant contributions to this study.

References

[1] S. Chaudhuri, S. Chatterjee, N. Katz, M. Nelson, and M. Goldbaum, "Detection of blood vessels in retinal images using two-dimentional matched filters," *IEEE Trans. Med. Img.,* vol. 8, no. 3, pp. 263-269 Sep. 1989.

[2] R. M. Rangayyan, F. J. Ayres, F. Oloumi, F. Oloumi, and P. Eshghzadeh-Zanjani, "Detection of blood vessels in the retina with multiscale Gabor filters," *J. Electron. Img.*, vol. 17, no. 2, 023018, Apr. 2008.

[3] M. Niemeijer, J. J. Staal, B. van Ginneken, M. Loog, and M. D. Abrámoff, "Comparative study of retinal vessel segmentation methods on a new publicly available database," in *Proc. SPIE: Med. Imag*. 2004, San Diego, 2004, vol. 5370, pp. 648–656.

[4] C. Muramatsu, Y. Hatanaka, T. Iwase, T. Hara, and H. Fujita, "Automated selection of major arteries and veins for measurement of arteriolar-to-venular diameter ratio on retinal fundus images," *Comput. Med. Imag. Graph*., vol. 35, no. 6, pp. 472–80, Sep. 2011.

[5] C. Muramatsu, A. Mizukami, Y. Hatanaka, A. Sawada, T. Hara, T. Yamamoto, and H. Fujita, "Improvement on recognition of major arteries and veins on retinal fundus images by template matching with vessel models," *Medical Imaging and Information Sciences*, vol. 30, no. 3, 63–69, Aug. 2013.

[6] M. Niemeijer, X. Xu, A. V, Dumitrescu, P. Gupta, B. van Ginneken, J. C. Folk, and M. D. Abrámoff, "Automated measurement of the arteriolar-to-venular width ratio in digital color fundus photographs," *IEEE Trans. Med. Imag*., vol. 30, no. 11, pp. 1941–1950, Nov. 2011.

[7] S. G. Vázquez, B. Cancela, N. Barreira, M. G. Penedo, M. Rodríguez-Blanco, M. Pena Seijo, G. Coll de Tuero, M. A. Barceló, M. Saez, "Improving retinal artery and vein classification by means of a minimal path approach," *Machine Vision and Applications*, vol. 24, no. 5, pp. 919–930, July 2013.

[8] C. Muramatsu, T. Nakagawa, A. Sawada, Y. Hatanaka, T. Hara, T. Yamamoto, and H. Fujita, "Automated segmentation of optic disc region on retinal fundus photographs: comparison of contour modeling and pixel classification methods," *Comput. Methods Programs Biomed.*, vol. 101, no. 1, 23–32, Jan. 2011.

[9] M. D. Knudtson K. E. Lee, L. D. Hubbard, T. Y. Wong, R. Klein, and B. E. K. Klein, "Revised formulas for summarizing retinal vessel diameters," *Current Eye Research*, vol. 27, no. 3, pp. 143–149, Sep. 2003.

[10] A. V. Stanton B. Wasan, A. Cerutti, S. Ford, R. Marsh, P. P. Sever, S. A. Thom, and A. D. Hughes, "Vascular network changes in the retina with age and hypertension," *J. Hypertens*, vol. 13, no. 12, pp. 1724–1728, Dec. 1995.

[11] T. Menzies and Y. Hu, "Data mining for very busy people," *IEEE Computer*, vol. 36, no. 11, pp. 18-25, Oct. 2003.

[12] Y. Hatanaka, K. Samo, M. Tajima, K. Ogohara, C. Muramatsu, S. Okumura, and H. Fujita, "Automated blood vessel extraction using local features on retinal images," in *Proc. SPIE Med. Imag. 2016*, San Diego, 2016, vol. 9785, pp. 97852F-1–-7.

[13] H. Tachiki, Y. Hatanaka, S. Okumura, K. Ogohara, R. Kawasaki, K. Saito, C. Muramatsu, and H. Fujita, "Semi-automated measurement of blood vessel diameter for arteriosclerosis retinae classification," in *Proc. Internat. Workshop Advanced Image Technology 2016*, Busan, 2016, paper P.1A-1.